1995A&A...294...23M

Astron. Astrophys. 294, 23–32 (1995)

ASTRONOMY
AND
ASTROPHYSICS

# Dense gas in nearby galaxies

## VIII. The detection of OCS

**R. Mauersberger**[1], **C. Henkel**[1], **and Y.-N. Chin**[2]

[1] Max-Planck-Institut für Radioastronomie, Auf dem Hügel 69, D-53121 Bonn, Germany
[2] Radioastronomisches Institut der Universität Bonn, Auf dem Hügel 71, D-53121 Bonn, Germany

Received 3 May 1994 / Accepted 29 July 1994

**Abstract.** The detection of extragalactic OCS, the heaviest molecule identified outside the Galaxy, is reported in three rotational transitions toward the bulge of NGC 253. Toward M 82, OCS has been tentatively detected. Abundances are consistent with models for warm, dense clouds which have not yet reached chemical equilibrium or with the frequent erosion of grain mantles by C-shocks. This can also explain the large abundances of complex molecules in NGC 253.

Densities and temperatures of the OCS emitting gas are compared with results from other molecular tracers. From model computations, OCS in the center of NGC 253 is emitted by a moderately dense molecular component with $n(H_2) \sim 10^{3.4}\mathrm{cm}^{-3}$. This component makes up the bulk of the molecular gas mass. Other molecules also reveal the presence of a much denser component with $10^{5-5.5}\mathrm{cm}^{-3}$. A molecular gas mass of $\sim 2\,10^8\,M_\odot$ is estimated for a 180 pc sized molecular cloud toward the center of NGC 253; the *mean* $H_2$ density is $\sim 2000\,\mathrm{cm}^{-3}$; and the mean $H_2$ column density, $7\,10^{23}\,\mathrm{cm}^{-2}$, corresponds to a visual extinction of $700^\mathrm{m}$. The relative OCS abundance is $X(\mathrm{OCS}) \sim 10^{-8.9}$.

From detections of the $J = 2 - 1$ and $3 - 2$ transitions of $C^{34}S$, the density of the dense molecular gas toward the nuclear region of IC 342 is $n(H_2) \sim 10^{4.6}\mathrm{cm}^{-3}$. Also presented are a possible detection of the $HC_3N$ $J = 16 - 15$ line toward IC 342 and upper limits for the emission of the DCN $J = 2 - 1$ line toward NGC 253 and IC 342. For NGC 253, [DCN]/[HCN] $\leq 4\,10^{-3}$.

**Key words:** ISM: molecules – galaxies: ISM – galaxies, individual: NGC 253, M 82, IC 342 radio lines: galaxies

### 1. Introduction

OCS (carbonyl sulfide) is among the most common sulfur-bearing molecules observed toward warm molecular clouds; toward the Orion Compact Ridge and Plateau, its abundance is slightly higher than that of CS (Blake et al. 1987). Since OCS is, however, much heavier than CS, its rotational energy can spread its population over more energy levels. Therefore, and due to its comparably low dipole moment of 0.72 Debye (Poynter & Pickett 1984), its lines are much weaker than those of CS, a molecule that is frequently used as a tracer of Galactic and extragalactic dense molecular gas. Detected for the first time in 1979 by Jefferts et al. (1971) in the interstellar medium, OCS has been used as a density probe toward warm and cold molecular cloud cores (Goldsmith & Linke 1981; Brown & Cragg 1985; Matthews et al. 1987). Chemical models (Millar & Herbst 1990) indicate that the abundance of OCS with respect to $H_2$ is much more time dependent than that of CS or SO. Therefore, observations of this molecule can test the idea that the high abundances of complex molecules toward NGC 253, and to a lesser degree toward M 82, may result from frequent destruction and reorganization of cloud features in the potential of galactic bulges.

In order to provide an independent tool for the estimation of densities, and to measure the abundance of another sulfur-bearing molecule in a starburst environment, we have searched for OCS emission in three galaxies and have detected this molecule toward NGC 253, and tentatively toward M 82.

### 2. Observations

The measurements of three different rotational lines of OCS and of two rotational lines of $C^{34}S$ were carried out in October 1993 using the IRAM 30-m telescope. Our non-detection of the DCN $J = 2 - 1$ line toward NGC 253 is based on observations made in summer 1990.

The line frequencies and beamwidths are displayed in Table 1. We have measured simultaneously the $J = 8 - 7$ with the $11 - 10$ line of OCS, and the $J = 2 - 1$ with the $3 - 2$ line of $C^{34}S$. The SIS receivers with a typical upper sideband rejection of 6 dB yielded system temperatures (on a main-beam brightness temperature scale ($T_{\mathrm{MB}}$)) between 330 and 500 K at $\lambda = 3$ and 2 mm. The data were calibrated using a chopper wheel. All intensities are given on a $T_{\mathrm{MB}}$ scale (Mauersberger

*Send offprint requests to*: R. Mauersberger

© European Southern Observatory • Provided by the NASA Astrophysics Data System

1995A&A...294...23M



**Table 1.** Observing parameters

| Transition | Frequency (GHz.) | $\theta_{beam}$ (arcsec.) |
|---|---|---|
| OCS (8 – 7) | 97.3012 | 25 |
| OCS (11 – 10) | 133.7859 | 17 |
| OCS (12 – 11) | 145.9468 | 16 |
| $HC_3N$ (16-15) | 145.5609 | 16 |
| $H_2CO$ ($2_{0,2} - 1_{0,1}$) | 145.6030 | 16 |
| $C^{34}S$ (2 – 1) | 96.4130 | 25 |
| $C^{34}S$ (3 – 2) | 144.6171 | 16 |
| DCN ($J = 2 - 1$) | 144.8280 | 16 |
| $^{12}CO$ (2 – 1) | 230.5380 | 12 |

et al. 1989), assuming beam efficiencies of 0.63 at $\lambda$ =3 mm, 0.56 at 2 mm and 0.45 at 1.3 mm. The spectra were taken using a wobbling secondary mirror with a switch cycle of 4 seconds (2 s on-source, 2 off-source). As a consequence mostly baselines of order zero, and in a few cases of order one, were subtracted. As backends we used filterbanks with 512 contiguous channels and 1 MHz width. The pointing was checked by continuum cross scans through nearby pointing calibrators with a 3 mm Schottky receiver. We also monitored the shape of the 2 – 1 line of $^{12}CO$ at 1 mm, which is very sensitive to deviations of the telescope pointing. The pointing did not vary by more than 3″. From measurements of the continuum of Saturn, the receivers used were aligned within 3″.

## 3. Results

We have detected OCS in three rotational transitions, namely in the $J = 8 - 7$, 11 – 10, and 12 – 11 lines toward the center of NGC 253. We show the profiles together with the coadded spectrum of $^{12}CO$ $J = 2 - 1$ in Fig. 1.

We have carefully checked the line catalog by Lovas (1992) and find that there are no strong lines from other molecular species that may blend with the OCS emission. There is line emission from the upper (image) sideband that can be assigned to $HC_3N$ ($J = 11 - 10$) near the OCS 8 – 7 profile. Because of the high rejection of radiation from this image band, calibration for this line is very uncertain. Therefore no fit results are given in Table 2. In the band containing the OCS 12 – 11 line, but at distinct velocities, there is comparably strong emission from the $2_{0,2} - 1_{0,1}$ line of $H_2CO$ and from the $J = 16 - 15$ line of $HC_3N$. To obtain the line parameters we have fitted Gaussian profiles to the spectra. The results are presented in Table 2. To improve the quality of the fit and to get a reliable estimate of the line intensity, we have in some cases fixed the linewidth (FWHM), $\Delta v_{1/2}$, and radial velocity (with respect to the Local Standard of Rest), $v_{LSR}$, to the values obtained from fits to the $^{12}CO$ $J = 2 - 1$ profile.

Toward the SW molecular hotspot of M 82, we may have detected the 8 – 7 and 11 – 10 transitions; only an upper limit can be given for the intensity of the 12 – 11 line. The latter is, however, located at the edge of our spectral band, which causes

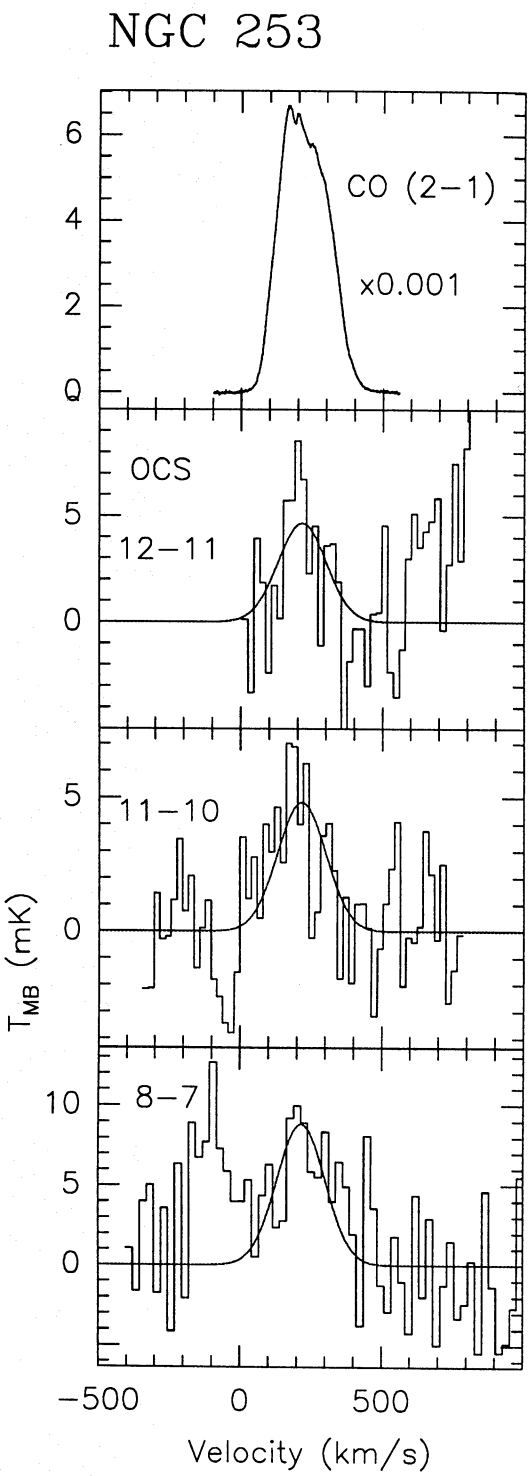


**Fig. 1.** Profiles of three rotational transitions of OCS toward the center of NGC 253 ($\alpha_{1950} = 0^h45^m6\overset{s}{.}0$, $\delta_{1950} = 25°33'36''$). For a comparison, the profile of the $^{12}CO$ $J = 2 - 1$ line is shown in the upper panel. The spectral resolution has been smoothed to approximately 20 km s$^{-1}$, except for CO, where it is 0.8 km s$^{-1}$. The velocity is with respect to the local standard of rest (LSR), the intensity scale is in main-beam brightness temperature. Gaussian fits to the profiles are drawn onto the spectra. The emission at −100 km s$^{-1}$ in the lower frame arises from the $J = 11 - 10$ line of $HC_3N$ in the upper (image) sideband of the receiver, and the strong emission near 1000 km s$^{-1}$ in the OCS 12 – 11 spectrum is the combined emission from lines of $H_2CO$ and $HC_3N$

© European Southern Observatory • Provided by the NASA Astrophysics Data System

1995A&A...294...23M



**Table 2.** Line parameters from Gaussian fits

| Source | Transition | $\int T_{MB} dv$ [a] | $T_{MB}$ | $v_{LSR}$ [b] | $\Delta v_{1/2}$ [b] | $T_B$ [c] |
|---|---|---|---|---|---|---|
| | | K km s$^{-1}$ | mK | km s$^{-1}$ | km s$^{-1}$ | mK |
| **NGC 253** | OCS 8 – 7 | 1.9(0.3) | 8.8(1.4) | *215* | *200* | 54(9) |
| | OCS 11 – 10 | 1.0(0.15) | 4.8(0.7) | *215* | *200* | 16(2) |
| | OCS 12 – 10 | 1.0(0.35) | 4.6(1.6) | *215* | *200* | 14(5) |
| | DCN $J = 3 - 2$ | $< 1$ [e] | $< 5$ | *215* | *200* | $< 15$ |
| | $HC_3N$ 16 – 15 [d] | $\sim 6$ | $\sim 30$ | *215* | *200* | $\sim 90$ |
| | $H_2CO$ $2_{0,2} - 1_{0,1}$ [d] | $\sim 10$ | $\sim 50$ | *215* | *200* | $\sim 160$ |
| | $^{12}CO$ 2 – 1 | 1450 | 6800 | 215 | 200 | 15000 |
| **M 82 SW** | OCS 8 – 7 | 1.2(0.3)? | 3.4(0.9) | 122(50) | 340(80) | |
| | OCS 11 – 10 | 0.4(0.1)? | 1.5(0.4) | 75(33) | 230(60) | |
| | OCS 12 – 11 | $< 0.5$ | | *144* | *97* | |
| | $HC_3N$ 16 – 15 [d] | | | | | |
| | $H_2CO$ $2_{0,2} - 1_{0,1}$ [d] | ~2.0 | 19 | *144* | *97* | |
| | $^{12}CO$ 2 – 1 | 725 | 7000 | 144 | 97 | 15000 |
| **IC 342** | OCS 12 – 11 | $< 0.15$ | | *32* | *55* | |
| | $C^{34}S$ 2 – 1 | 0.73(0.19) | 15(4) | 21(7) | 45(16) | 90(25) |
| | $C^{34}S$ 3 – 2 | 0.74(0.12) | 16(2) | 25(4) | 43(9) | 50(6) |
| | DCN 2 – 1 | $< 0.15$ | | *32* | *55* | |
| | $HC_3N$ 16 – 15 | 0.3(0.1) | 8(3) | 24(5) | 39(11) | 25(9) |
| | $H_2CO$ $2_{0,2} - 1_{0,1}$ | 1.0(0.1) | 20(2) | 26(2) | 46(4) | 62(6) |
| | $^{12}CO$ 2 – 1 | 160 | 2700 | 32.1 | 55 | 6000 |

a) Errors, given in parenthesis, are standard deviations from Gaussian fits and do not include uncertainties due to calibration, which we estimate to be 10 – 15%.
b) Parameters which have been fixed in the Gaussian fitting are printed in italics.
c) Calculated brightness temperature if the emission arises in a 10″ sized Gaussian source and were measured with a 12″ beam.
d) Blended.
e) From rms in 80 km$^{-1}$ wide channels.

some uncertainty in the determination of the baseline. Profiles are shown in Fig. 2.

The line widths of the features at the OCS 8 – 7 and 11 – 10 frequencies seem to be much broader than the $^{12}CO$ 2 – 1 line. This *might* be caused by the larger beam at 3 mm and 2 mm wavelengths, which also picks up emission from regions with different radial velocity. In view of the non-detection of 12 – 11 emission and the differences in line shape, the identification of OCS toward M 82 is tentative, at best. To obtain the line parameters of the $HC_3N$ and $H_2CO$ emission, we fixed velocity and line width to the values obtained from $^{12}CO$. It appears that the emission comes mainly from $H_2CO$. Because of line blending we do not give an upper limit to the intensity of the $HC_3N$ $J = 16 - 15$ line in Table 2.

For IC 342, we present detections of the $J = 2 - 1$ and 3 – 2 lines of $C^{34}S$, and upper limits to the OCS 12 – 11 line (which is located at the edge of our spectrometer bandpass) and the $J = 2 - 1$ line of DCN (Fig. 3). The values for the upper limits in Table 2 are $1\sigma$ values obtained from Gaussian fits with $v_{LSR}$ and $\Delta v_{1/2}$ fixed to the values obtained from $^{12}CO$. Since IC 342 has a comparably small linewidth, $HC_3N$ and $H_2CO$ can be well separated toward this source. From the intensity of $HC_3N$, and assuming similar excitation of this molecule as toward NGC 253 (Mauersberger et al. 1990), $N(HC_3N) \sim 5\ 10^{13}$ cm$^{-2}$.

## 4. Model computations

To model the OCS emission, we have used a large-velocity gradient non-LTE statistical equilibrium model. Thirteen rotational levels were taken into account. The collision rates have been adopted from Green & Chapman (1978). Line trapping reduces the effective speed of radiative processes in a cloud by a factor $\beta$, the photon escape probability. For a spherical geometry, which is assumed for our model, $\beta = (1 - \exp(-\tau))/\tau$.

For a comparison with model computations, we have to convert the main-beam brightness temperatures obtained from Gaussian fits to source averaged brightness temperatures, $T_B$. For this purpose, one has to make some assumptions about the geometry of the line emitting regions.

In a CO map of NGC 253, Canzian et al. (1988) identified two molecular spots, each with a size of slightly more than 10″. Also from a single dish map of $^{12}CO$ where the spatial resolution has been improved by a Lucy deconvolution (Mauersberger et al., in preparation), the 200 km s$^{-1}$ component has a size of $\sim 10''$ and is spatially separated from an emission hotspot with a radial velocity of 300 km s$^{-1}$. These components can also be

© European Southern Observatory • Provided by the NASA Astrophysics Data System

1995A&A...294...23M



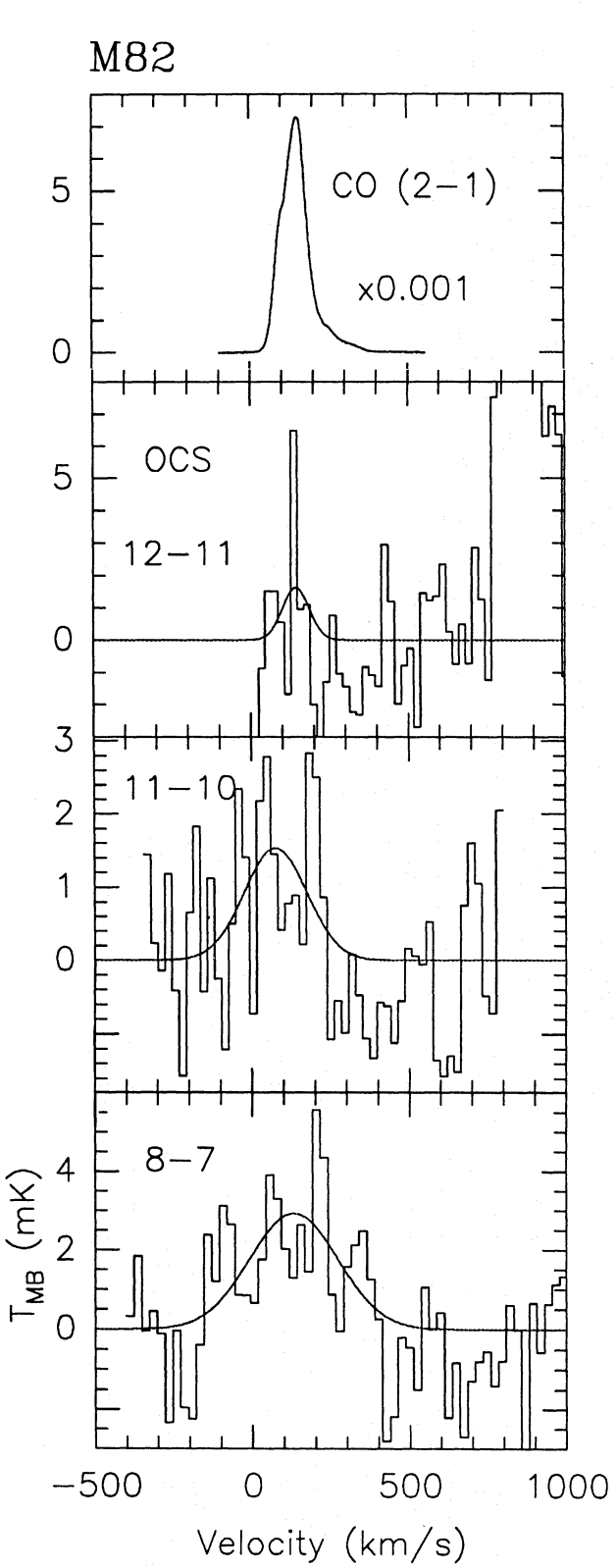


**Fig. 2.** OCS and $^{12}$CO spectra toward the SW molecular hotspot of M 82, which is located at $(\Delta\alpha, \Delta\delta) = (-10'', -10'')$ relative to $\alpha_{1950} = 9^h51^m43^s.0$, $\delta_{1950} = 69°55'00''$, the center of the galaxy. The spectral resolution has been smoothed to 20 km s$^{-1}$, except for CO, where it is 0.8 km s$^{-1}$. The strong emission near 1000 km s$^{-1}$ in the OCS 12 – 11 spectrum is the combined emission from lines of $H_2CO$ and $HC_3N$

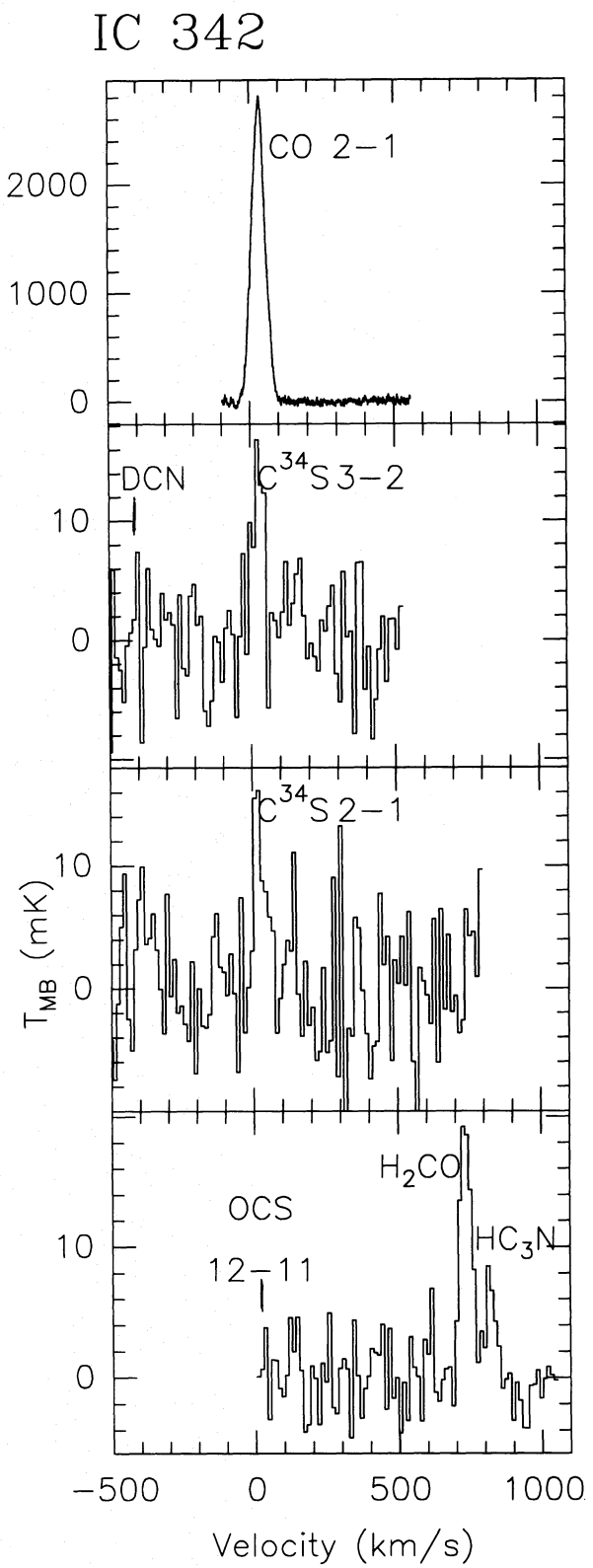


**Fig. 3.** $H_2CO$ $2_{02} - 1_{01}$ and $HC_3N$ 16 – 15 profiles toward the center of IC 342 ($\alpha_{1950} = 3^h41^m57^s.5$, $\delta_{1950} = 67°56'27''$). The OCS 12 – 11 line, which should peak near 30 km s$^{-1}$, is not detected. Also profiles of $^{12}$CO (upper panel), and two transitions of $C^{34}S$ are shown. The frequency of the $J = 2 - 1$ transition of DCN is indicated. The spectral resolution has been smoothed to $\sim$ 12 km s$^{-1}$, except for the CO profile, where the velocity resolution is 0.8 km s$^{-1}$

© European Southern Observatory • Provided by the NASA Astrophysics Data System

1995A&A...294...23M



identified from two distinct velocity components in spectra of $CH_3OH$ and $HC_3N$ taken with a beam of 26″ (Henkel et al. 1987; Mauersberger et al. 1990), which show a double-horned profile. Data with higher resolution can spatially separate these components. Since we have forced the fitted Gaussians toward NGC 253 to have the same shape and velocity as our high resolution $^{12}CO$ spectrum, our fit results give the line intensities for the molecular hotspot at 200 km s$^{-1}$ only.

Toward M 82 there are two molecular hotspots of size $\sim$ 10″, which are spatially and kinematically well separated. (Carlstrom 1988).

Downes et al. (1992) detected five HCN emitting cloud cores toward the center of IC 342. These are grouped within a circle of 10 – 15″ in diameter. The beam of the IRAM 30-m telescope cannot distinguish between the cloud cores but collects radiation from all five cores. Therefore the relevant "source size" for the 30-m telescope is that of the central group of cores.

To be consistent with the interferometer data and with Mauersberger & Henkel (1989) and Mauersberger et al. (1990) we shall assume that the OCS and $C^{34}S$ lines toward NGC 253, IC 342, and also M 82 are emitted from Gaussian-shaped regions with a size of $\theta_s$ =11″. If $\theta_b$ is the beam width, the source averaged brightness temperature is given by $T_B = T_{MB}(\theta_s^2 + \theta_b^2)/\theta_s^2$. In the last column of Table 2, we give values for $T_B$ for those lines that have been unambiguously identified and detected.

We have measured only three transitions of OCS. Two of these, namely the $J$ = 12 – 11 and the 11 – 10 lines have very similar excitation conditions, and as a consequence, have nearly the same intensity. Therefore, we use the measured *ratios* of source averaged brightness temperatures, $T_B$, for the 8 – 7 line and the 11 – 10 line (which has a smaller uncertainty than the 12 – 11 transition) to constrain the physical parameters of the OCS emitting gas toward NGC 253. This ratio is $T_B(8-7)/T_B(11-10)$ = 3.4 (±1.0). We have also assumed that the OCS lines are optically thin. This is suggested by Galactic multilevel studies (e.g. Brown & Cragg 1985). In this case, the line intensity *ratios* are not influenced by line trapping and do not depend on the velocity gradient and the molecular column density but in essence only on the $H_2$ density and, to a lesser degree, on the kinetic temperature.

The results of our OCS model computations are plotted in Fig. 4. If NGC 253 has a kinetic temperature of 60 K, which is plausible from $NH_3$ studies for the bulk of the gas toward IC 342 and our Galactic center (Martin & Ho 1986; Mauersberger et al. 1986), our model can be reconciled with the observations if the $H_2$ density of the OCS emitting gas in NGC 253 is $10^{3.4\pm0.2}$ cm$^{-3}$. If the kinetic temperature is as low as 30 K, the density is a factor 1.4 higher. The column density of OCS averaged over an 11″ source size is 5 $10^{15}$ cm$^{-2}$.

If the excitation of OCS is similar toward NGC 253, M 82 and IC 342, the 1$\sigma$ OCS column density limits are $N$(OCS) $\leq$ 5 $10^{14}$ cm$^{-2}$ for an 11″ source toward M 82, and $N$(OCS) $\leq$ 8 $10^{13}$ cm$^{-2}$ for an 11″ region in the center of IC 342.

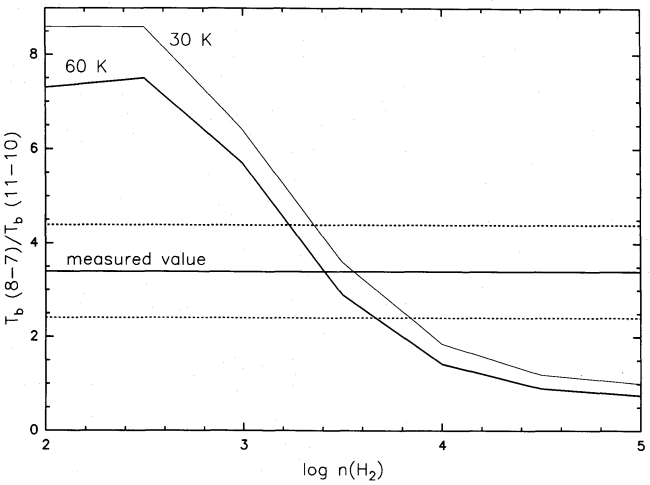


**Fig. 4.** OCS $J$ = 8 – 7/$J$ = 11 – 10 intensity ratios versus $H_2$ density for two values of $T_{kin}$ as obtained for optically thin lines from an LVG model simulating a spherical homogeneous cloud. The OCS line intensity ratio, and its errors, actually determined toward NGC 253 is also plotted

## 5. Excitation and the physical state of the gas

### *5.1. The physical state of the dense gas toward NGC 253*

A number of molecules have been observed in several transitions toward the center of NGC 253, allowing multilevel studies to investigate the physical state of the gas. While CO is commonly the most thoroughly investigated molecular species, the present CO data base for NGC 253 is not sufficient for detailed density models (Güsten et al. 1993). Galactic studies with a comparably high linear resolution show that the interstellar medium is far from being homogeneous. There is not only clumping on various scales (cf. Wilson & Walmsley 1989), but also different chemical abundances in different regions (e.g. Goldsmith et al. 1987). Therefore, it is expected that also toward the nuclear environment of external galaxies, there is more than just one gas component. For NGC 253, this has been confirmed from multilevel studies of CS and $HC_3N$ (Mauersberger & Henkel 1989; Mauersberger et al. 1990).

How do the results from these different density tracers compare for NGC 253? In order to investigate this question we compile the results from six molecules in Table 3. Besides the molecular column density and the $H_2$ density, we also give the value of the molecular dipole moment, on which the "critical" density depends, which is a frequently used but crude estimate of the local $H_2$ density if no multilevel data are available. The spontaneous decay rate for the rotational transition between levels $J$ + 1 and $J$ in a linear molecule is

$$A_{ul} = \frac{64\pi^4\mu^2\nu^3}{3hc^3} = 1.2\,10^{-11}\mathrm{s}^{-1}\left(\frac{\mu_0}{\mathrm{Debye}}\right)^2\left(\frac{\nu}{\mathrm{GHz}}\right)^3\frac{J+1}{2J+3}. \quad (1)$$

$\mu_0$ is the molecular dipole moment. In many cases, molecules are excited by collisions with $H_2$ molecules. The corresponding collision rate is given by $C = n < \sigma v >$ . Here, $\sigma$ is

© European Southern Observatory • Provided by the NASA Astrophysics Data System

1995A&A...294...23M



**Table 3.** Parameters of the molecular gas toward galactic bulges

| Tracer | $\mu_0$ Debye | levels | $N^a$ cm$^{-2}$ | log $X^b$ | $n^c_{crit}$ cm$^{-3}$ | $n(H_2)$ cm$^{-3}$ | comment[d] |
|---|---|---|---|---|---|---|---|
| **NGC 253** | | | | | | | |
| CO | 0.1 | 5 | $7\,10^{19e)}$ | −4 | $10^{3.2}-10^{5.5}$ | $10^4-10^5$ | (1,6) |
| CS | 2.0 | 3 | $5\,10^{15}$ | −8.2 | $10^{5.5}-10^{6.8}$ | $10^4$+$10^{5.4}$ | also $C^{34}S$ measured (2) |
| $HC_3N$ | 3.7 | 6 | $5.5\,10^{14}$ | −9.2 | $10^{5.8}-10^{7.3}$ | $10^4$+$10^{5.7}$ | (3) |
| $CH_3CCH$ | 0.75 | 5 | $6\,10^{14}$ | −9.1 | $10^{4.5}-10^{5.9}$ | $10^{4.5}$ | (4) |
| $CH_3CN$ | 3.9 | 5 | $8\,10^{13}$ | −10.0 | $10^{6.0}-10^{7.3}$ | $10^{4.8}$ | (4) |
| $H_2CO$ | 2.3 | 2 | | | | $10^5-10^{5.5}$ | (5) |
| OCS | 0.72 | 3 | $1.0\,10^{15}$ | −8.9 | $10^{4.7}-10^{5.2}$ | $10^{3.4}$ | (6) |
| **M 82** | | | | | | | (1) |
| CO | 0.1 | 5 | $4\,10^{19e)}$ | −4 | $10^{3.2}-10^{5.5}$ | $10^3$+$10^5$ | (1,6) |
| CS | 2.0 | 3 | $1\,10^{15}$ | −8.6 | $10^{5.5}-10^{6.8}$ | $10^4$+$10^{5.4}$ | also $C^{34}S$ measured (2) |
| $CH_3CCH$ | 0.75 | 5 | $5\,10^{14}$ | −8.9 | $10^{4.5}-10^{5.9}$ | $10^{4.5}$ | (4) |
| $CH_3CN$ | 3.9 | 5 | $<2\,10^{13}$ | $<-10.3$ | $10^{6.0}-10^{7.3}$ | | (4) |
| **IC 342** | | | | | | | |
| CO | 0.1 | 5 | $8\,10^{18e)}$ | −4 | $10^{3.2}-10^{5.5}$ | $10^3$+$10^{4.3}$ | (1,6) |
| CS | 2.0 | 3 | $2.6\,10^{14}$ | −8.5 | $10^{5.5}-10^{6.8}$ | $10^{4.6}$ | also $C^{34}S$ measured (2,6) |

a) column density averaged over an 11″ source size

b) assuming an $H_2$ column density (averaged of a source size of 11″) of $7.4\,10^{23}$ cm$^{-2}$ for NGC 253; $3.7\,10^{23}$ cm$^{-2}$ for M 82, and $0.8\,10^{23}$ cm$^{-2}$ for IC 342

c) critical density of the lowest and highest transition involved

d) (1) Güsten et al. (1993); (2) Mauersberger & Henkel (1989); (3) Mauersberger et al. (1990); (4) Mauersberger et al. (1991); (5) Baan et al. (1990); (6) this paper

e) from $X(CO)=10^{-4}$ (Frerking et al. 1982) and obtaining $N(H_2)$ from our CO spectra and the conversion formula of Strong et al. (1988).

the collisional cross section, and $v$ is the velocity of the $H_2$ molecules. For a kinetic temperature of 60 K typical values are $C \sim 6\,10^{-11}\,s^{-1}\frac{n(H_2)}{cm^{-3}}$ (Green & Chapman 1978) for the molecules and transitions considered here. Setting the spontaneous decay rate of a transition equal to the collision rate yields the *critical density*,

$$n_{crit} \sim 0.1\,(\mu_0/\mathrm{Debye})^2\,(\nu/\mathrm{GHz})^3. \quad (2)$$

It can be seen from Table 3 that higher densities are predicted from studies involving transitions with higher critical densities. In all the cases, however, the transitions are subcritically excited, i.e. $n(H_2) << n_{crit}$ and $T_{ex} << T_{kin}$. This means that the bulk of the emission arises from lower density gas. From the data, we can conclude that all the studies can be reconciled if there are two molecular density components, the first one with $n(H_2) \sim 10^{3.5}$–$10^{4.5}$ cm$^{-3}$ and the second one with $n(H_2) \sim 10^5$–$10^{5.5}$ cm$^{-3}$. Alternatively there can be a continuous distribution of densities in the beam. Obviously the gas components with densities surpassing $10^5$ cm$^{-3}$ are the candidates for star formation in the near future.

In order to calculate relative abundances from the molecular column densities given in Table 3, we have to know the source averaged column density of $H_2$. This can be obtained using our measurement of the CO $J = 2-1$ line intensity toward the center of NGC 253 and the "standard" factor determined by Strong et al. (1988) for the $J = 1 - 0$ line of CO:

$$N(H_2)/I_{CO} = 2.3\,10^{20}\,\mathrm{cm}^{-2}/(\mathrm{K\,km\,s}^{-1}). \quad (3)$$

A similar ratio for the $J = 2 - 1$ line of CO has not been determined systematically. Braine et al. (1993) investigated a number of spiral galaxies and find that, on the average, this line is a factor 0.9 weaker than the $1 - 0$ transition. Assuming that this also holds for NGC 253, the beam averaged $H_2$ column density along the line-of-sight is $3.7\,10^{23}$ cm$^{-2}$, and if all the emission in the beam arises from an 11″ sized source, the source-averaged column density becomes $7.4\,10^{23}$ cm$^{-2}$. If the standard $A_V/E_{B-V}$ relation (Bohlin et al. 1978) can be applied to the bulge region of NGC 253, an $H_2$ column density of $7\,10^{23}$ cm$^{-2}$ corresponds to a mean visual extinction of 700$^m$. This extinction may be patchy.

From the interferometric study by Canzian et al. (1988), the *average* column density over a 39″ × 12″ molecular bar is $3\,10^{22}$ cm$^{-2}$. From these data, Mauersberger & Henkel (1989) estimated that the column density averaged over the main intensity peak (assumed size: 11″) is $1.5\,10^{23}$ cm$^{-3}$. Since our CO $2-1$ measurement has been observed with the same instrument as the other density tracers presented in Table 3, we will use the $H_2$ column density determined from the 30-m telescope for a determination of relative abundances.

© European Southern Observatory • Provided by the NASA Astrophysics Data System

1995A&A...294...23M



At a distance of 3.4 Mpc (Sandage & Tammann 1975), a source size of 11″ corresponds to a linear size of 180 pc. From our CO column density, the total molecular mass in our beam, including helium and metals, is 2.5 $10^8$ $M_\odot$. Assuming a spherical source geometry, the *mean* $H_2$ density is 2000 $cm^{-3}$. This is very similar to the value obtained from our OCS multilevel study and would imply that the volume filling factors of the CO and OCS emitting gas are close to unity. Another hint in favor of a high molecular beam filling factor is the high brightness temperature of CO averaged over an assumed 11″ sized region; it is $\sim$ 15 K in the 2 – 1 line. At densities $\gtrsim$ 2000 $cm^{-3}$, brightness temperatures of CO are predicted to be 25–45 K if the CO emission is optically thick and if $T_{kin}$ is between 30 and 60 K. Hence, the area filling factor of the CO emission should be in the range 30-50%.

### 5.2. Dense gas toward IC 342

The spiral galaxy IC 342 is only 10° from the Galactic plane. Without the high extinction caused by Galactic dust, it would be one of the brightest galaxies in the sky. Recently, McCall (1989) found that it is located nearer than previously believed, namely at 1.8 Mpc. That makes it a rather normal galaxy with a gas content and infrared luminosity similar to the corresponding values of our Milky Way.

Here, we present measurements of $C^{34}S$, which supply information which was missing in the CS multilevel study of Mauersberger & Henkel (1989) and which allows to determine the density of the CS emitting gas. Main isotopic CS lines are often optically thick (e.g. Linke & Goldsmith 1980). A comparison of the intensity of the $C^{32}S$ emission with that from $C^{34}S$ yields a quantitavie estimate on $\tau$ since $C^{34}S$ is almost certainly optically thin and since the Galactic isotope ratio $^{32}S/^{34}S \sim 23$ (Wannier 1980) may also be applicable to IC 342.

The $C^{32}S/C^{34}S$ intensity ratios of source averaged brightness temperatures toward the position of IC 342 measured here are 5.1 and 5.7 for the $J = 2-1$ and $3-2$ lines. This corresponds to optical depths of $\tau = 4.5-5$ in the main isotope's lines. From the $NH_3$ multilevel study by Martin & Ho (1986) the kinetic temperature of the dense gas is $\gtrsim$ 50 K. Using the model described by Mauersberger & Henkel (1989), with the intensity ratio of $C^{34}S$, $\frac{T_B(2-1)}{T_B(3-2)} = 1.8(\pm 0.7)$, the $H_2$ density of the CS emitting gas is in the optically thin case $n(H_2) = 10^{4.6\pm0.5}$ $cm^{-3}$ (see Fig. 7a of Mauersberger & Henkel 1989). A CS brightness temperature of $\sim$ 8 K is predicted at such a density and a kinetic temperature of 60 K. If the clouds are virialized by their own gravity, it can be shown (see e.g. Downes et al. 1993) that for any optically thick emission line, the total gas mass (in solar masses, including He and metals) is given by $M_{gas} = 2.6\, T_{MB} \Delta v_{1/2} A_B \sqrt{n(H_2)}/T_B$. Here $T_{MB}$ is the main-beam brightness temperature (in Kelvin) averaged over a beam with an area $A_B$ (in pc). If we insert the corresponding values for CS emission from Mauersberger & Henkel (1989), we find that the observed CS emission represents a gas mass of 6 $10^6$ $M_\odot$. This is in excellent agreement with the estimate from the five HCN emitting clumps detected by Downes et al. (1992) and is $\sim$ 20% of the total mass in molecular clouds in the central 20″ of IC 342 obtained from the CO luminosity by Eckart et al. (1990) and the conversion factor by Strong et al. (1988).

From our model calculations, the column density of CS (averaged over an 11″ source size) is 2.6 $10^{14}$ cm. From our CO line intensity measurement, the column density of $H_2$ toward the same region is 0.8 $10^{23}$ $cm^{-2}$, in good agreement with Eckart et al. (1990). In this case $X(CS) = 3\,10^{-9}$. This is compatible with abundances in Galactic molecular clouds, which are $10^{-7.8} \ldots 10^{9.0}$ (Guélin 1988).

## 6. Chemical implications

### 6.1. Extragalactic sulfur chemistry

OCS is the third sulfur-bearing molecule detected toward extragalactic objects after CS (Henkel & Bally 1985) and SO, which has been detected toward NGC 253 and, marginally, toward M 82 (Petuchowski & Bennett 1992). According to Millar & Herbst (1990), the main reactions producing OCS at intermediate densities ($\gtrsim 10^4$ $cm^{-3}$) are

$$CO + S \rightarrow OCS + h\nu \quad (4)$$

and

$$O + HCS \rightarrow OCS + H. \quad (5)$$

These authors have modelled the abundances of sulfur bearing molecules for a cloud resembling the Orion ridge for an early phase in the chemical evolution (32000 yrs) and for steady state.

While CS and SO abundances may only vary by factors of 0.25 and 2.5 between early and steady state chemistry, the abundance of OCS is predicted to be highly time variable: at the early state an abundance of $10^{-9}$ is calculated. This value drops dramatically to 2 $10^{-11}$ when chemical equilibrium is reached. Our value of $10^{-8.9}$ determined for NGC 253 can be explained by a non-equilibrium chemistry. Due to frequent cloud collisions and shocks in the very confined bulge region of galaxies such as NGC 253 it is possible that the clouds have no time to reach chemical equilibrium. OCS abundances as high as $10^{-9}$ seem, however, to be normal for a wide variety of Galactic molecular clouds, such as dark clouds and Giant Molecular clouds (Goldsmith & Linke 1981; Matthews et al. 1987), and it is not very likely that none of those clouds should have reached chemical equilibrium.

It has been proposed that non-equilibrium chemistry could also explain the large amounts of complex molecules such as $CH_3CCH$ or $CH_3CN$ (Herbst & Leung 1989), which are abundant in NGC 253 (Mauersberger et al. 1991). With new reaction rates, the early-time abundance peaks seem, however, to be less pronounced (Herbst et al. 1994). High abundances of some molecular species such as methanol toward Hot Cores are also predicted by the evaporation from grain mantles (Brown et al. 1988). Flower et al. (1994) showed that C-shocks are not only capable to heat large amounts of molecular gas to high temperatures; they can also evaporate grain mantles perhaps explaining the rich molecular chemistry in galactic bulge regions.

© European Southern Observatory • Provided by the NASA Astrophysics Data System

1995A&A...294...23M



Cosmic rays, have also been proposed to modify interstellar chemistry (Farquhar et al. 1994). If these would be, however, the main heating source of the warm gas in galactic bulge clouds, they would easily dissociate fragile molecules (Hüttemeister et al. 1994). 5.6 eV are, e.g., sufficient to destroy HCN (Allen 1991).

### *6.2. Chemical abundances toward galactic and extragalactic cloud cores*

Due to our higher estimate of the $H_2$ column density toward NGC 253, the molecular abundances relative to $H_2$ ($X$) in Table 3 are lower than the values obtained by Mauersberger et al. (1991) which were based on the $N(H_2)$ value by Canzian et al. (1988). As a consequence, relative molecular abundances of NGC 253 and M 82 become more similar. We compare the revised values of relative abundances toward M 82, NGC 253 and IC 342 in Fig. 5.

Since $H_2$ column density determinations depend on our confidence in a universal $N(H_2)/I_{CO}$ conversion factor, the relative abundances of different high density tracing molecules, e.g., $N(OCS)/N(CS)$, may be a much more reliable indicator of molecular chemistry.

The relative abundance of OCS seems to be much more constant in the interstellar medium than, e.g. the abundances of methanol or ammonia. For giant molecular clouds and for dark clouds such as TMC 1, $X(OCS)$ is a few times $10^{-9}$ (Goldsmith & Linke 1981; Matthews et al. 1987), while enhanced values of $> 10^{-8}$ are observed toward Sgr A, Sgr B2 or the Orion Plateau source (Blake et al. 1987; Minh et al. 1992). Our value determined toward NGC 253, $X(OCS) \sim 10^{-9}$, is within the range found in the Galactic interstellar medium. Let us, however, recall that the linear size of our beam is much larger than any map of Galactic OCS. This, and the fact that, in spite of its lower dipole moment, OCS seems to be spatially more concentrated than e.g. $HC_3N$ (Goldsmith et al. 1987), suggests that OCS abundances may be locally much higher than our beam averaged value.

This may also be true for other molecules in Fig.5. If one compares the chemical mixtures of different galaxies, the over-abundances of SiO and $CH_3OH$ in NGC 253 when compared with M 82 are among the noteworthy pecularities (for a discussion, see Henkel & Mauersberger 1992). The scatter in relative abundances of different molecules between different galaxies is on the same order as that between Sgr A and Sgr B2 (Minh et al. 1992) or within Sgr B2 (Goldsmith et al. 1987). It seems that NGC 253 possesses a richer chemistry than M 82.

### *6.3. Deuterated molecules in galactic bulges*

From our non-detections of deuterated HCN toward IC 342 and NGC 253, we can estimate the abundance of DCN relative to HCN. This is straight forward only for NGC 253 toward which $HC^{13}N$ has been observed (Mauersberger & Henkel 1991), which is almost certainly optically thin, while HCN, which has been observed toward both NGC 253 and IC 342 (Nguyen-Q-Rieu et al. 1992), is thought to be optically thick.

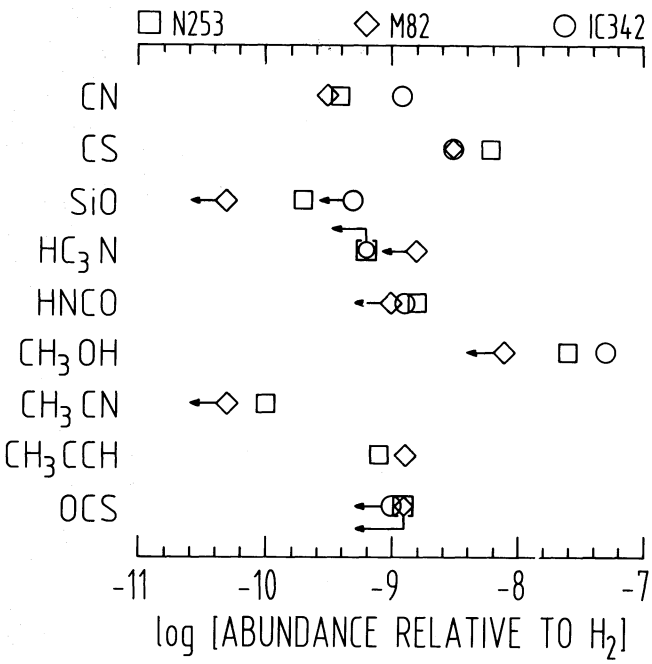


**Fig. 5.** Abundances relative to $H_2$ for a number of molecules in the direction of the dense molecular cores surrounding the nuclei of M 82, NGC 253 and IC 342. Note that, due to our revised estimate on $N(H_2)$ for NGC 253, relative molecular abundances are lower than estimated before. The data used are from this paper (OCS, $HC_3N$, $H_2$), from Henkel et al. (1988: CN, $HC_3N$; 1989: $CH_3OH$), Mauersberger & Henkel (1989: CS; 1991: SiO), Mauersberger et al. (1990: $HC_3N$, 1991: $CH_3CCH$, $CH_3CN$), Nguyen-Q-Rieu et al. (1991: HNCO), Hüttemeister (1993: $CH_3OH$ in M 82)

The estimated $1\sigma$ brightness temperature ratio between the $J = 1 - 0$ line of $H^{13}CN$ and the $2 - 1$ line of DCN toward NGC 253 (deconvolved for a source size of $11''$) is $R = T_B(DCN)/T_B(H^{13}CN) \leq 0.11$.

In the Appendix, we show that $N(H^{13}CN)/N(DCN) \sim 1.5\,R$. From this, $N(DCN)/N(H^{13}CN) \leq 0.17$. Since Henkel et al. (1993) find that $N(H^{12}CN)/N(H^{13}CN) \sim 40$ for the center of NGC 253, we estimate that $N(DCN)/N(H^{12}CN) \leq 4\,10^{-3}$. For IC 342, $H^{13}CN$ has not been measured, but we estimate that the limit on $N(DCN)/N(H^{12}CN)$ is similar to the value given for NGC 253.

While the cosmic [D]/[H] abundance ratio is as low as $1.6\,10^{-5}$, a number of deuterium bearing molecules are enriched in the interstellar medium. This does not only hold for cold clouds, for which such a fractionation is theoretically predicted, but it may also be valid for hot molecular cores (e.g. Jacq et al. 1990). The degree of fractionation varies, however, not only from cloud to cloud but also from molecule to molecule. For [DCN]/[HCN], Schilke et al. (1992) find values as high as $10^{-3}$ toward the Orion Hot Core and $0.01 - 0.06$ in the ridge, which they can explain by steady state chemical models as long

© European Southern Observatory • Provided by the NASA Astrophysics Data System

1995A&A...294...23M



as $T_{kin} < 50$ K. Other explanation involve the evaporation of grain mantles.

Observations summarized by Penzias (1980) suggest a ratio of $10^{-3}$ for [DCN]/[HCN] toward the Galactic center, but this analysis is based on noisy data. From a detection of HDO in the Sgr B2 molecular core, Jacq et al. (1990) conclude that the degree of fractionation is of the same order as toward other hot hores. Our limit on [DCN]/[HCN] toward NGC 253 is comparable to the ratio measured toward Sgr B2. A large abundance of DCN is, however, even less expected for NGC 253 than for our Galactic center in view of the massive star formation in this galaxy, which (1) effectively destroys deuterium and (2) precludes the presence of cold molecular gas.

## 7. Conclusions

Our main conclusions are:

1. We have detected carbonyl sulfide (OCS) toward the center of the starburst galaxy NGC 253, and tentatively toward M 82. OCS is the heaviest molecule and the third sulfur bearing compound detected outside the Milky Way. In NGC 253, it is emitted from a region of moderate $H_2$ density, $n(H_2) \sim 10^{3.4}$ cm$^{-3}$. From a comparison with other molecular tracers, the bulk of the $H_2$ is at such a moderate density while a smaller fraction of the gas has a density two orders of magnitudes higher.
   A molecular gas mass of $2.8\,10^8$ M$_\odot$ is estimated for the inner 180 pc of NGC 253; the *mean* $H_2$ density is $\sim 2000$ cm$^{-3}$. The mean column density of $7\,10^{23}$ cm$^{-2}$ corresponds to a mean visual extinction of 700$^m$.
2. The high abundance of OCS relative to $H_2$, $X(OCS) = 10^{-8.9}$, could indicate that OCS emitting clouds toward the bulge of NGC 253 are in an early state of chemical evolution.
3. The detection of two transitions of $C^{34}S$ toward IC 342 allows to estimate the density of the CS emitting component to be $n(H_2) = 10^{4.6}$ cm$^{-3}$ and $X(CS) = 3\,10^{-9}$. This dense phase makes up 20% of the mass of a less dense and more extended molecular component.
4. From a non-detection of DCN toward the center of NGC 253 [DCN]/[HCN]$\leq 4\,10^{-3}$. This limit is much higher than the cosmic [D]/[H] ratio, but lower than ratios found toward some Galactic cloud cores.

*Acknowledgements.* We thank the referee, Prof. P. M. Solomon, for valuable comments.

## Appendix A: an estimate of the [HCN]/[DCN] abundance ratio

In the optically thin case and if the excitation temperature $T_{ex} >> 2.7\,K$, the total molecular column density is

$$N(\mathrm{mol}) = 8.52\,10^{12}\,\mathrm{cm}^{-2}\mu^{-2}\frac{2J+1}{J}\frac{k}{h\nu}f_J^{-1}\int T_B \mathrm{d}v \qquad (6)$$

(e.g. Schilke et al. 1992) for a transition $J \rightarrow J-1$, at a frequency $\nu$. The dipole moment $\mu$ is in Debye and the integrated intensity in K km s$^{-1}$. $f_J$ denotes the fraction of $N_{mol}$ which is at state $J$. From this equation,

$$\frac{N(\mathrm{DCN})}{N(\mathrm{H^{13}CN})} = 0.5\,\frac{f_1(\mathrm{HC^{13}N})}{f_2(\mathrm{DCN})}R, \qquad (7)$$

where $R$ is the line intensity ratio between $H^{13}CN$ $(1-0)$ and DCN $(2-1)$. From model computations by Schilke (1992) we find that for densities $n(H_2) = 10^{5-6}$ cm$^{-3}$, and in the optically thin case, $\frac{f_1(\mathrm{HC^{13}N})}{f_2(\mathrm{DCN})} \sim \frac{0.45}{0.15} \sim 3$, and we obtain

$$\frac{N(\mathrm{DCN}}{N(\mathrm{H^{13}CN})} \sim 1.5\,R. \qquad (8)$$

## References


Allen, C.W., 1991, Astrophysical Quantities, The Athlone Press, London

Baan, W.A., Henkel, C., Schilke, P., Mauersberger, R., Güsten, R., 1990, ApJ 353, 132

Blake, G.A., Sutton, E.C., Masson, C.R., Phillips, T.G., 1987, ApJ 315, 621

Bohlin, R.C., Savage, B.D., Drake, J.F., 1978, ApJ 224, 132

Braine, J., Combes, F., Casoli F. et al., 1993, A&AS 97, 887

Brown, P.D., Charnley, S.B., Millar, T.J., 1988, MNRAS 231, 409

Brown, R.D., Cragg, D.M., 1985, MNRAS 215, 395

Canzian, B., Mundy, L.G., Scoville, N.Z., 1988, ApJ 333, 157

Carlstrom, J.E., in: Galactic and Extragalactic Star Formation, eds. R.E. Pudritz, M. Fich, Kluwer, p.571

Downes, D., Radford, S.J.E., Guilloteau, S., Guélin, M., Greve, A., Morris, D., 1992, A&A 262, 424

Downes, D., Solomon, P.M., Radford, S.J.E., 1993, ApJ 414, L13

Eckart, A., Downes, D., Genzel, R. et al., 1990, ApJ 348. 434

Farquhar, P.R.A., Millar, T.J., Herbst, E., 1994, MNRAS, in press

Flower, D.R., Pineau des Forêts, G., Walmsley, C.M., 1994, A&A, in press

Frerking, M.A., Langer, W.D., Wilson, R.W., 1982, ApJ 262, 590

Goldsmith, P.F., Linke, R.A., 1981, ApJ 245, 482

Goldsmith, P.F., Snell, R.L., Hasegawa, T., Ukita, N., 1987, ApJ 314, 525

Green, S., Chapman, S., 1978, ApJS 37, 169

Guélin, M., 1988 in "Molecules in Physics, Chemistry and Biology", Vol. II., ed.: J. Maruani, Kluwer Academic Publ., p. 175

Güsten, R., Serabyn, E., Kasemann, C. et al., 1993, ApJ 402, 537

Henkel, C., Jacq, T., Mauersberger, R., Menten, K.M., Steppe, H., 1987, A&A 188, L1

Henkel, C., Mauersberger, R., 1992, IAU Symp. 150 "Astrochemistry of Cosmic Phenomena", ed.: P. Singh, Kluwer Academic Publishers, Dordrecht, p.111

Henkel, C., Mauersberger, R., Schilke, P., 1988, A&A 201, L23

Henkel, C., Mauersberger, R., Wiklind, T. et al., 1993, A&A 268, L17

Herbst, E., Lee, H.H., Howe, D.A., Millar, T.J., 1994, MNRAS 268, 335

Herbst, E., Leung, C.M., 1989, ApJS 69, 271

Hüttemeister, S., 1993, PhD Thesis, Bonn University

Hüttemeister, S., Wilson, T.L., Mauersberger, R. et al., 1994, A&A, in press

Jacq, T., Walmsley, C.M., Henkel, C., Baudry, A., Mauersberger, R., Jewell, P.R., 1990, A&A 228, 447

Jefferts, K.B., Penzias, A.A., Wilson, R.W., Solomon, P.M., 1971, ApJ 168, L111


© European Southern Observatory • Provided by the NASA Astrophysics Data System

1995A&A...294...23M



Linke, R.A., Goldsmith, P.F., 1980, ApJ 235, 437
Lovas, F.J., 1992, J. Phys. Chem. Ref. Data 21, 181
Martin, R.N., Ho, P.T.P., 1986, ApJ 308, L7
Matthews, H.E., MacLeod, J.M., Broten, N.W., Madden, S.C., Friberg, P., 1987, ApJ 315, 646
Mauersberger, R., Guélin, M., Martín-Pintado, J., Thum, C., Cernicharo, J., Hein, H., Navarro, S., 1989, A&AS 79, 217
Mauersberger, R., Henkel, C., 1989, A&A 223, 79
Mauersberger, R., Henkel, C., 1991, A&A 245, 457
Mauersberger, R., Henkel, C., 1993, Rev. Modern Astron. 6, 69
Mauersberger, R., Henkel, C., Sage, L.J., 1990, A&A 236, 63
Mauersberger, R., Henkel, C., Walmsley, C.M., Sage, L.J., Wiklind, T., 1991, A&A 247, 307
Mauersberger, R., Henkel, C., Wilson, T.L., Walmsley, C.M., 1986, A&A 162, 199
McCall, M.L., 1989, AJ 97, 1341
Millar, T.J., Herbst, E., 1990, A&A 231, 466
Minh, Y.C., Irvine, W.M., Friberg, P., 1992, A&A 258, 489
Nguyen-Q-Rieu, Henkel, C., Jackson, J.M., Mauersberger, R., 1991, A&A 241, L33
Nguyen-Q-Rieu, Jackson, J.M., Henkel, C., Truong-Bach, Mauersberger, R., 1992, ApJ 399, 521
Penzias, A.A., 1980, Science 208, 663
Petuchowski, S.J., Bennett, C.L., 1992, ApJ 391, 137
Poynter, R.L., Pickett, H.M., 1984, Submillimeter, millimeter and microwave spectral line catalog, JPL Publ. 80-23
Sandage, A., Tammann, G.A., 1975, ApJ 196, 313
Schilke, P., 1992, PhD Thesis, Bonn University
Schilke, P., Walmsley, C.M., Pineau des Forêts, G., Roueff, E., Flower, D.R., Guilloteau, S., 1992, A&A 256, 595
Strong, A.W., Bloemen, J.B.G.M., Dame, T.M., Lebrun, F. et al., A&A 207, 1
Swade, D.A., Schloerb, F.P., 1992, ApJ 392, 543
Wannier, P.G., 1980, ARA&A 18, 399
Wilson, T.L., Walmsley, C.M., 1989, ARA&A 1, 141

This article was processed by the author using Springer-Verlag LaTeX A&A style file version 3.

© European Southern Observatory • Provided by the NASA Astrophysics Data System